ELSEVIER

Contents lists available at ScienceDirect

Journal of Sea Research

journal homepage: www.elsevier.com/locate/seares



Limited effects of UVBR on primary productivity and photosynthetic pigment composition in the Greenland Sea

Malin Olofsson a,*, Sten-Åke Wängberg b, Anna Engelsen c, Angela Wulff c,*

- a Department of Aquatic Sciences and Assessment, Swedish University of Agricultural Sciences, Box 7050, 750 07 Uppsala, Sweden
- ^b Department of Marine Sciences, University of Gothenburg, Box 461, 405 30 Göteborg, Sweden
- ^c Department of Biological and Environmental Sciences, University of Gothenburg, Box 463, 405 30 Göteborg, Sweden

ARTICLE INFO

Keywords: Primary productivity Climate change Arctic Photosynthetic pigments UV-absorbing compounds Sea ice retreat

ABSTRACT

The Arctic icescape currently undergoes major transformations along with anthropogenic perturbations and climate change. These changes are affecting phytoplankton community composition and primary productivity in a possibly synergistic manner. With less ice, the phytoplankton communities will experience elevated light conditions, and there is a need to understand how low-light adapted phytoplankton species react to changes in light composition including ultraviolet B radiation (UVBR 280-320 nm) exposure. We therefore look back two decades (May 2002) in order to expand the limited but necessary baseline for comparative field observations of primary productivity and phytoplankton pigment composition, comparing under ice to open water conditions, and UVBR exposure to shielded conditions. Along the East Greenland Current cruise transects we observed a large patchiness in primary productivity, with indications of under-ice blooms with chlorophyll a values up to 9.9 μ g l⁻¹, nitrate concentration < 0.1 μ M, and primary productivity of 11.7 μ g C l⁻¹ h⁻¹. Surprisingly, we only observed a minor effect of UVBR treatment on primary productivity, and we did not observe a difference in mycosporine-like amino acids (MAAs) in the plankton community samples at surface (2 m) and deeper (approx. 20 m) water depths. Due to its early onset of climate related effects, studies in the Arctic region may signal future changes of ecosystems at lower latitudes. This comprehensive dataset on primary productivity, UV-absorbing compounds (MAAs), and pigment composition could offer a valuable baseline for assessing ecological change. It can inform climate impact modelling, support long-term ecosystem monitoring, and hopefully guide future management strategies in this vulnerable marine environment.

1. Introduction

Climate change and anthropogenic perturbations are affecting all ecosystems on the planet, and the Arctic ecosystem is warming two to four times faster as compared to the rest of the globe (Rantanen et al., 2022; Yamanouchi and Takata, 2020), thus, the Intergovernmental Panel on Climate Change announces it as highly vulnerable (IPCC, 2023). IPCC further predicts changes in timing, duration, and intensity of primary production along with the ongoing climate changes (Meredith et al., 2019). With elevated air and surface water temperatures, the Arctic ice-system will become seasonal rather than perennial within 50 years (Wassmann and Reigstad, 2011), and less ice may prolong the phytoplankton growth period (Lebrun et al., 2019; Manizza et al., 2023). Already, the Greenland ice sheet has experienced substantial ice loss over the recent two decades (King et al., 2020). Changes

in the ice coverage is also part of the reason why increased net primary production rates have been observed in the Arctic Ocean since the 1990s (Arrigo and van Dijken, 2015) as well as in the Barents and Kara Sea (Renaut et al., 2018). A rapidly changing environment is expected for the Arctic region phytoplankton communities with potential consequences for the Arctic food-web (Renaud et al., 2024), yet knowledge on how this will affect primary productivity is still limited and we lack a baseline for comparisons.

Changes in the Arctic ice coverage affect the light climate (Neale et al., 2023) and taxa of primary producers have an optimum light range for photosynthesis without experiencing light-stress (Platt et al., 1982). Thus, increased light penetration in Arctic aquatic ecosystems may impose additional stress on phytoplankton communities adapted to low-light conditions beneath the ice (Lund-Hansen et al., 2020). On the other hand, persistently low light can itself act as a physiological stressor, and

E-mail addresses: malin.olofsson@slu.se (M. Olofsson), angela.wulff@bioenv.gu.se (A. Wulff).

^{*} Corresponding authors.

increased light availability may enhance photosynthetic performance and overall productivity (Castellani et al., 2022). Another potential threat is exposure to UVBR penetrating the water column due to declining snow and ice cover. Microplankton demonstrate a wide range of responses to UVBR, with some species exhibiting high sensitivity to damage while others are less sensitive or possess robust repair mechanisms (Bouchard et al., 2005; Wängberg et al., 2008; Leu et al., 2016). Some taxa of phytoplankton produce UV-absorbing compounds, mostly mycosporine-like amino acids (MAAs), with absorbance in the UVR spectrum 310–360 nm (Carreto et al., 2005).

The satellite-based models estimating increased net primary production rates (Arrigo and van Dijken, 2015; Renaut et al., 2018), have limitations, and in situ measurements are needed to quantify primary productivity under the ice. This is because the primary production potential of natural phytoplankton communities under in situ environmental conditions is otherwise not accounted for, nor is the composition of the phytoplankton community. For in situ measurements aimed at estimating integrated values, certain assumptions will be required, each carrying its own limitations. Pabi et al. (2008) presents a formula for integrated primary production which includes light availability as a function of depth, chlorophyll (chl) a, growth rate, time and temperature, based on a model from Arrigo et al. (2008). This way the estimates capture several of the natural variations in abiotic and biotic features of different water masses. In 2013, a synthesis of primary productivity in the Arctic was published, pointing out that rate measurements were scarce and sporadic (Matrai et al., 2013).

We previously published data on microplankton biodiversity and community composition in the East Greenland Current (EGC) in the same survey as herein, from 2002 (AO-02; Olofsson and Wulff, 2021). In relation to that dataset, we now present a large dataset of primary productivity in relation to UVBR exposure, phytoplankton pigment composition and MAAs from the same cruise. The present study dates two decades back with the aims of: I) providing a baseline of primary productivity measurements in relation to pigment composition, MAAs and ice presence across largely variable conditions, as well as II) determine the effect of UVBR-stress on primary productivity in incubation experiments using natural microplankton communities, and III) model the diurnal and depth integrated primary production and estimate the effect of elevated temperatures, based on *in situ* measurements and light profiles.

2. Material and methods

2.1. The expedition Arctic Ocean 2002

The Swedish icebreaker Oden covered the East Greenland Current from the north of Fram Strait to the south of Denmark Strait, as part of the Arctic Ocean 2002 programme (AO-02). The expedition was conducted April to June 2002, started from north of Svalbard and followed the east coast of Greenland (82°14′ N to 64° 46′ N). This region has an arctic climate with sea ice coverage during winter and spring (Fig. 1). For more details on the physicochemical parameters during the same cruise, AO-02, see e.g., Nilsson et al. (2008) and Rudels et al. (2005), and Olofsson and Wulff (2021) for microplankton community composition and biodiversity parameters.

2.2. Sea water sampling and light measurements

The samplings for this paper were conducted between the 1st and 26th of May along nine transects with a total of 56 stations (Fig. 1 and Table 1). The transects started from the ocean towards the ice-covered coastline. Since Oden is an icebreaker, we were able to sample with the ship breaking through the ice as we progressed. Air temperature ranged between -30° and 0 $^\circ\text{C}$ and water temperature between $-1.82\,^\circ\text{C}$ and 6.61 $^\circ\text{C}$ (Table 1). Salinity ranged between 32 and 35 PSU, with low variation between surface and deep samples suggesting a well-

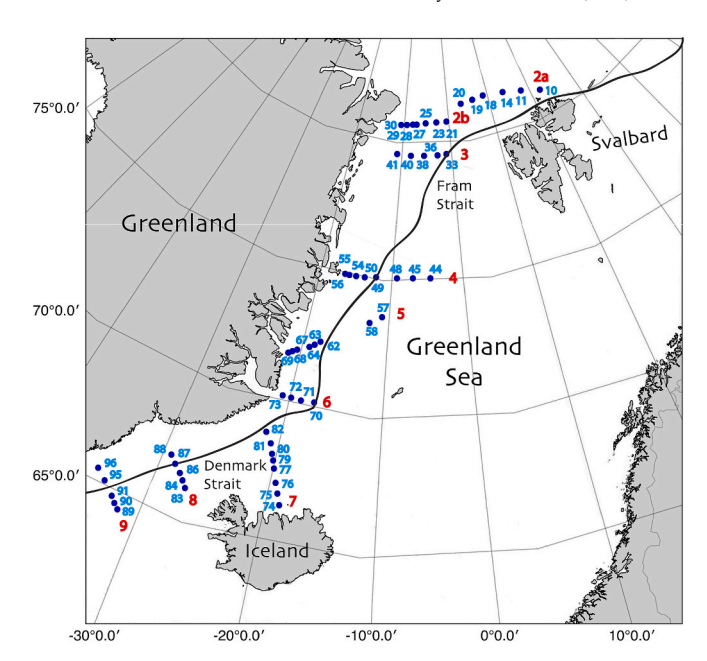


Fig. 1. Expedition map for transects 2a, 2b, 3, 4, 5, 6, 7, 8, and 9, including station numbers in light blue, starting from the ocean heading towards the coastline of Greenland. The black line indicates the ice-edge (ice maps retrieved from the Danish Meteorological Institute for May 2002). (For interpretation of the references to colour in this figure legend, the reader is referred to the web version of this article.)

mixed Upper Mixed Layer (UML), and lowest values close to the ice edge. Measurements of salinity and temperature were obtained using a CTD SBE 911plus instrument (see Rudels et al., 2005).

Since the main CTD unit lacked a fluorometer, a smaller handheld CTD equipped with a fluorometer was used to determine the depth of the fluorescence maximum. As soon as the research vessel had come to a stop and ice conditions allowed, the handheld CTD was deployed. Based on the fluorescence data obtained, we identified the depth from which to collect water samples using the main CTD rosette. Seawater was generally sampled from two depths: the surface (2 m depth), hereafter referred to as "surface," and from the chl a maximum layer (typically 15-50 m), hereafter referred to as "deep." If the chl a maximum could not be determined, samples were instead taken at 20 m depth (details for sampling depths in Table 1). Seawater for sample collection or incubation experiments was collected in dark bottles, from the SeaBird Carousel rosette sampler (12 l Niskin bottles) or from GoFlo sampling bottles. Immediately after water collection, filtration for pigment analysis and incubations for primary productivity were started. Photosynthetically active radiation intensity (PAR 400-700 nm) in the air (on deck) was measured using a light meter (International Light 1400 A) equipped with a PAR sensor (IL SEL033) and generally coincided with incubations for primary productivity. Underwater light attenuation curves were attained by vertical PUV-500 (Biospherical Instruments, San Diego, USA) measurements for 6 stations (14, 20, 23, 33, 40, 58). Four discrete wavelengths (305, 320, 340 and 380 nm) and PAR were measured, each measurement was done from the surface to ca 50 m and from 50 m back to the surface with 1 m resolution. The average value for each meter was used.

2.3. Measured primary productivity

At 33 of the stations, surface and deep water was collected using the rosette sampler (depths in Table 1). Subsamples of 10 ml were pipetted into 20 ml scintillation vials (Packard, high quality), and 20 μl of $H^{14}CO_3^-$ (5 $\mu Ci)$ was added to each vial. The vials were sealed and incubated in a laboratory container for 4 h at 90 μmol photons m^{-2} s $^{-1}$

Table 1
Station details including transect, station number, sampling date (YYMMDD), surface/deep water temperature (°C), surface/deep salinity, sampling depth, ice presence, and coordinates, ND = no data.

Transect	Station	Date	Temperature	Salinity	Sampling depth (m)	Ice presence	Coordinates
2a	10	02-05-01	-1.58/-1.55	34.38/34.38	2/20	Ice-covered	81.00 N, 18.22 E
	11	02-05-01	-1.57/-1.46	34.26/34.28	10/20	Ice-covered	81.13 N, 18.11 E
	14	02-05-02	-1.82/-1.81	34.36/34.36	2/20	Ice-covered	81.38 N, 16.06 E
	18	02-05-03	-1.82/-1.82	34.33/34.33	2.5/20	Ice-covered	82.15 N, 06.55 E
	19	02-05-03	-1.83/-1.83	34.33/34.33	2/20	ND	82.23 N, 05.58 E
	20	02-05-04	-1.86/-1.86	34.29/34.29	2/20	Thin ice	82.21 N, 03.06 E
2b	21	02-05-06	-1.85/-1.85	34.39/34.39	2/20	Thick ice	81.30 N, 00.02 W
	23	02-05-07	-1.83/-1.83	33.97/34.00	2/20	Thick ice	81.26 N, 04.09 W
	25	02-05-09	-1.71/-1.71	32.00/32.01	2/20	Thin ice	81.22 N, 07.16 W
	27	02-05-09	-1.72/-1.72	31.95/31.95	2/20	ND	81.26 N, 08.37 W
	28	02-05-09	-1.71/-1.71	31.97/31.97	2/20	ND	81.16 N, 08.22 W
	29	02-05-09	-1.70/-1.72	32.00/32.01	2/20	ND	81.27 N, 08.97 W
	30	02-05-09	-1.72/-1.74	31.97/31.99	2/20	ND	81.18 N, 08.57 W
3	33	02-05-12	-1.74/-1.74	34.14/34.14	2/30	Ice-covered	79.18 N, 00.03 W
	36	02-05-13	-1.65/-1.67	32.66/32.72	2/20	Thin ice/open water	79.10 N, 03.58 W
	38	02-05-13	-1.74/-1.75	32.48/32.48	2/15	Ice-covered	79.00 N, 05.25 W
	40	02-05-14	-1.77/-1.76	32.60/32.60	2/20	Thick ice	79.01 N, 08.06 W
	41	02-05-14	-1.75/-1.75	32.52/32.52	2/20	Ice-covered	78.97 N, 09.95 W
4	44	02-05-16	-0.52/-0.59	34.85/34.85	2/20	Open water	75.00 N, 01.93 W
•	45	02-05-16	-0.42/-0.41	34.86/34.86	2/30	Open water	74.99 N, 04.01 W
	48	02-05-17	0.22/0.10	34.81/34.84	6/50	Open water	75.00 N, 09.30 W
	49	02-05-17	0.49/0.65	34.76/34.83	2/40	Ice-edge	75.00 N, 10.73 W
	50	02-05-17	-0.16/0.25	34.53/34.72	2/35	ND	74.99 N, 11.28 W
	54	02-05-17	-0.10/0.23 -1.82/-1.82	34.30/34.30	2/20	Mostly covered	74.96 N, 12.89 W
	55	02-05-18	-1.82/-1.82 -1.74/-1.73		2/20	Ice with holes	75.00 N, 14.30 W
	56	02-05-18		33.52/33.67		ND	
-			-1.78/-1.79	33.44/33.53	2/10		75.60 N, 15.25 W
5	57 58	02-05-19	-0.11/-0.15	34.67/34.67	2/20	Open water	73.50 N, 10.00 W
		02-05-19	0.37/0.33	34.72/34.72	2/16	Open water	73.25 N, 12.00 W
	62	02-05-20	-1.77/-1.79	34.12/34.16	2/10	Ice with holes	72.55 N, 16.83 W
	63	02-05-20	-1.79/-1.79	33.65/33.66	2/20	ND	72.28 N, 17.28 W
	64	02–05-20	-1.75/-1.75	33.85/33.89	2/20	ND	72.38 N, 18.20 W
	67	02–05-21	-1.78/-1.78	32.86/32.88	-/20	ND	72.08 N, 19.50 W
	68	02–05-21	-1.73/-1.71	32.68/32.71	2/20	ND	72.00 N, 21.02 W
_	69	02–05-21	-1.72/-1.77	32.64/32.73	2/20	Ice with leads	71.95 N, 21.38 W
6	70	02–05-24	-1.82/-1.82	33.74/22.74	2/20	Drifting ice	70.00 N, 20.24 W
	71	02–05-24	-1.83/-1.83	33.76/33.76	2/20	Thick ice	70.00 N, 20.83 W
	72	05-05-25	-1.79/-1.79	32.84/32.84	2/20	ND	70.00 N, 21.51 W
	73	02-05-25	-1.77/-1.77	32.72/32.72	2/20	ND	70.00 N, 22.02 W
7	74	02-05-26	-1.78/-1.78	32.85/32.86	2/20	ND	69.61 N, 21.83 W
	75	02-05-26	-1.81-1.81	33.52/33.53	2/20	Thick ice, few holes	69.35 N, 21.49 W
	76	02-05-26	-1.73/-1.81	33.77/33.84	2/20	ND	69.09 N, 21.24 W
	77	02-05-26	-1.63/-1.63	34.17/34.20	2/25	Open water	69.01 N, 21.23 W
	79	02-05-27	-0.27/-0.27	34.61/34.61	2/20	ND	68.16 N, 20.48 W
	80	02-05-27	1.26/1.23	34.67/34.67	2/18	Open water	67.77 N, 20.52 W
	81	02-05-27	3.53/3.57	34.84/34.84	2/20	Open water	67.20 N, 20.34 W
	82	02-05-27	2.84/2.77	34.70/34.70	2/20	ND	66.84 N, 20.00 W
8	83	02-05-28	5.67/5.67	35.07/35.07	2/20	Open water	66.26 N, 25.56 W
	84	02-05-28	6.62/6.41	35.09/35.09	2/20	ND	66.25 N, 25.53 W
	86	02-05-28	-1.26/-1.27	34.10/34.10	4/15	Open water	66.76 N, 26.78 W
	87	02-05-28	-1.53/-1.55	33.79/33.80	2/20	ND	66.58 N, 27.18 W
	88	02–05-28	-1.80/-1.82	33.38/33.56	2/20	Drifting ice, small holes	67.30 N, 28.14 W
9	89	02-05-29	6.61/6.60	35.08/35.08	2/20	Open water	64.77 N, 31.73 W
-	90	02-05-29	6.66/6.66	35.10/35.10	2/20	ND	64.59 N, 32.09 W
	91	02-05-29	6.31/6.32	35.06/35.06	2/20	Open water	65.19 N, 32.65 W
	95	02-05-30	-1.72/-1.71	32.94/32.95	2/20	Thick ice, few holes	65.77 N, 34.30 W
	96	02-05-30	-1.72/-1.71 -1.79/-1.80	33.02/33.02	2/10	Thick ice, lew noies	65.88 N, 34.73 W
	90	02-05-30	-1./9/-1.80	33.02/33.02	2/10	THICK ICE	03.00 N, 34./3 W

(PAR 400–700 nm) and 0.4 W m $^{-2}$ UVBR (280–320 nm) (corresponding to ca 2–5 m depth) and ice blocks were used to keep the temperature < 2 °C. The vials were mounted in an inverted position to minimize shading from the lids. Light sources for incubation were Osram L 36 W/72–965 Biolux (PAR) and Philips ultraviolet-B TL 20 W/12 RSF 20 T 12/UVB (UVBR). Three replicates from each sampling were exposed to UVBR or shielded using Mylar plastic film. To ensure equivalent light conditions across all incubations, flasks without Mylar plastic were covered with a neutral shading net that compensated for the light reduction caused by the Mylar. PAR was measured to confirm that all flasks received comparable intensities. All flasks were protected from UVCR using cellulose diacetate film. For spectra of plastic films and scintillation vials see Wängberg and Wulff (2004). Along with the light treatments, one sample was placed in a dark box to correct for dark

uptake.

After 4 h, 200 µl of 37 % formaldehyde was added to the vials to end the incubations and thereafter acidified with HCl to reach pH <2 and left with open lids on a shaking board overnight to dispose of inorganic carbon. New lids were thereafter added to avoid cross-contamination between samples. Scintillation cocktail (Beckman, Ready Gel) was added and the radioactivity (counts min $^{-1}$, CPM) was measured on a scintillation counter (Tri-carb 2100 TR Liquid Scintillation analyser). CPM was measured in blanks before the scintillation cocktail was added to make sure all the non-fixed carbon was removed. DPM (disintegration by minutes) was given from CPM values by applying a quench curve. DPM was thereafter converted to primary productivity (PP; µg C l $^{-1}$ h $^{-1}$) according to Ærtebjerg Nielsen and Bresta, 1984 using the formula:

$$PP = DPMa^*totCO2^*12^*1.05^*1.06/t^*DPMb$$

where $totCO_2$ is alkalinity multiplied with the F-factor (0.998) according to Parsons et al., 1984, 12 the atomic weight of carbon, 1.05 the correction factor of ^{14}C being heavier than ^{12}C , 1.06 correction factor of the respiration of organic matter at optimal photosynthesis (being 6 %), t being the incubation time in hours, DPM-a the measured DPM (average of three technical replicates) in a given sample (minus the DPM in the dark controls), and DPM-b the activity of added C^{14} . No volumetric conversion was needed as measurements were conducted in unamended concentration of the sea water. This method was recently described in Zdun et al. (2021). Stations where blanks had DPM values above obtained DPM values were considered lacking primary productivity at the time of sampling and therefore given a zero. As primary productivity rates were obtained from controlled on deck incubations they shall be seen as potential rates and not reflecting station-specific *in situ* conditions.

As primary productivity was significantly correlating with chl a (Fig. S1) we calculated chl a-specific productivity ($C \, chl^{-1} \, h^{-1}$) by dividing primary productivity ($\mu g \, C \, l^{-1} \, h^{-1}$) with chl a concentration ($\mu g \, l^{-1}$) (see pigments section for details on analysis). Chl a to carbon ratios are known to vary with light and nutrient availability, and average ratios in Barents Sea range between 0.01 and 0.04, thus, an average of 0.025 was used for conversion (Sakshaug et al., 2009). Thereby, the chl a concentrations were converted to community carbon concentrations ($\mu g \, C \, l^{-1}$) by using a factor of 40. Primary productivity was divided by the carbon concentrations to attain carbon-specific carbon-production (h^{-1}), and also calculated to estimated carbon-doubling times (days) by the formula 1/(carbon-specific carbon-production*24), assuming light availability 24 h per day.

Rough estimate of integrated production (mg C m $^{-2}$ d $^{-1}$) was calculated based on mg C l $^{-1}$ h $^{-1}*1000*24*10$, assuming continuous (24-h) primary production due to the absence of darkness and extending down to a depth of 10 m.

From the measured primary productivity, we calculated community carbon doubling time in days (the inverse of carbon production per day). The carbon doubling time was used to calculate carbon-based growth rates (\mathbf{d}^{-1}) by taking the inverse of the doubling time.

2.4. Diurnal and depth integrated primary production

To get an estimate of the diurnal depth integrated production we used the formula presented in Pabi et al. (2008) (Eq. (2)). Light depth profiles were measured by PUV (see methods for details) at 6 stations. To obtain diurnal two-dimensional (time and depth) estimates of light, we assumed the daily variation in surface radiation as described by Campbell and Norman (1998), and that the light attenuation in water, measured once, remained constant throughout the day. Secondly, diurnal integrated production (mg C m $^{-2}$ d $^{-1}$) was estimated as in Pabi et al. (2008):

$$PP = \int\limits_{z=0}^{100} \int\limits_{t=0}^{24} chl \ a(z) \frac{carbon}{chl \ a} G \Biggl(z, \ t \Biggr) dt dz \eqno(2)$$

where z = depth (m), carbon/chl a ratio (40 g/g, see discussion above), t = time (hour) and G = gross production calculated as:

$$G = G(z,t) = G_0[r^*T(t)]*L(z,t)]$$
(3)

where T = temperature (°C) and G_0 = nominal microalgal growth rate. For this we used values from incubation instead of the standard value 0.59 (based on Eppley, 1972) used in Arrigo et al. (2008) and Pabi et al. (2008). Further, r = rate constant (0.063 C⁻¹) that determines the sensitivity of G to temperature (T, °C) was based on Eppley (1972), and corresponds to a Q10-value of 1.88. We used the temperature measurements from the CTD. As a comparison we estimated productivity at

two constant temperatures (0 and $+\,2\,^{\circ}$ C). Further, L represents the light limitation term, and as primary productivity dependence on light intensity decreases at high light intensities, when factors other than light limit production, a spectral photo acclimation factor (E_k') is applied (Arrigo et al., 2008):

$$L(z, t) = 1 - \exp(-PAR(zt)/E_{k}(z, t))$$
(4)

We used PAR instead of PUR, where in equation 5 it is daily average at depth z. PUR equals to Photosynthetically Utilizable Radiation that was used in Arrigo et al. (2008). L was calculated for each depth and hour where:

$$E_{k}'(z, t) = E_{k_{max}}'/(1 + 2exp(-BPAR(z)))$$
 (5)

and

(1)

$$B = \exp(1.089 - 2.12 \log(E_{k \text{ max}}))$$
 (6)

where $E_{k'max}$ was set to 80 µmol photons m^{-2} s⁻¹. This is the maximum observed value for $E_{k'max}$ based on Arrigo et al. (1998) who compiled spectral irradiance data and corresponding values of $E_{k'}$ for phytoplankton collected over a wide range of times, depths, and locations in the Southern Ocean.

2.5. Photosynthetic pigment concentrations

For pigment analysis, 250-3000 ml of seawater from surface and deep samples (Table 1) was filtered onto GF/F filters, immediately (onboard) frozen in liquid nitrogen (-196 °C) and stored in -80 °C. Filtration took place in dim light at 4 °C to minimize the influence of light and temperature. For extraction, 1.5 ml of 100 % MeOH was added, and the extract was sonicated 30 s using a Vibra-cell sonicator equipped with a 3 mm diameter probe. The extraction and HPLC-analysis continued according to Wright and Jeffrey (1997) using an absorbance diode-array detector (Spectraphysics UV6000LP). The column used was a C18 Phenomenex Ultracarb 3 mm ODS (20) (150 \times 3.20 mm) and a guard column, SecurityGuard Phenomenex C18 (4 \times 3.0 mm). The HPLC system was calibrated with pigment standards from DHI Lab, Denmark. Peak identities were further confirmed by on-line recording of absorbance spectra (400-700 nm) as described in Wright and Jeffrey (1997). Detected and identified pigments were chlorophyll c_3 (chl c_3), chlorophyll $c_1 + c_2$ (chl c_1c_2), peridinin (perid), 19'-butanoyloxyfucoxanthin (19-but), fucoxanthin (fucox), 19'-hexanoyloxyfucoxanthin (19-hex), prasinoxanthin (prasin), violaxanthin (violax), diadinoxanthin (diadin), alloxanthin (allox), diatoxanthin (diatox), lutein, zeaxanthin (zeax), chlorophyll b (chl b), chlorophyll a, (chl a), alpha-carotene (b-car1) and beta-carotene (b-car2). Pigments are expressed as $\mu g l^{-1}$ and ratios to chl

2.6. Mycosporine-like amino acids (MAAs)

For analyses of MAAs, 250-3000 ml of seawater from surface and deep samples (Table 1) was filtered onto GF/F filters, immediately frozen onboard in liquid nitrogen (-196 °C) and stored in -80 °C. Filtration took place in dim light at 4 °C to minimize the influence of light and temperature. For extraction, 1.5 ml of 25 % MeOH was added and the extraction proceeded in a water bath at 45 °C for 2 h. After extraction, the suspension was analyzed using HPLC as follows: the gradient was 0 min 100 % solvent A, 0 % solvent B; 2 min 100 % solvent A, 0 % solvent B; 10 min 80 % solvent A, 20 % solvent B; 12 min 50 % solvent A, 50 % solvent B; 14 min 100 % solvent A, 0 % solvent B. Solvent A was water plus 2 ml TFA (pH 3.15), and solvent B was 80 % solvent A, 10 % MeOH and 10 % acetonitrile (ν/ν , pH 2.3). The column was a ChromTech AB Capcell Pak SG C18 150 \times 4.6 mm, 3 μm i.d., equipped with a guard column (SecurityGuard Phenomenex C18 (4 \times 3.0 mm). Flow rate 0.5 ml min⁻¹. The detector was an absorbance diodearray detector (Spectraphysics UV6000LP), and the peaks were identified by on-line recording of absorbance spectra (280–400 nm). Due to the lack of commercially available standards, concentrations of MAAs are expressed as absorbance units (area) to chl a (MAAs/chl a).

2.7. Statistical analyses

Pearson's correlation coefficient (r) and R^2 were used (Microsoft Excel ToolPak) to assess the strength and explained variance of the linear relationship between X and Y (pigments and MAAs). Statistical significance was set at p < 0.01 (n = 30–32 if not specified). Only statistically significant values are reported.

3. Results

3.1. Measured primary productivity and chl a

Primary productivity, measured in samples collected both from open water and under sea ice (Table 1), ranged from undetectable to $11.66~\mu g$ C l⁻¹ h⁻¹ (Table 2). The highest values were found at stations with high chl a concentrations and the highest rate was recorded in a sample comprising communities from an ice-covered station (Table 1). Chl a concentration and primary productivity were positively correlated (Fig. S1). *In situ* temperatures did not affect the measured primary productivity (incubated at similar temperature), as high rates were observed both in communities collected from stations with low (station 95 with $-1.7~^{\circ}$ C) and relatively higher temperatures (station 58 with $3.5~^{\circ}$ C). Neither did productivity correlate with species diversity (From Olofsson and Wulff, 2021; Pearson correlation coefficient of -0.27, $R^2 = 0.07$, n = 17) nor with sea ice presence (Fig. S2).

The highest chl a concentrations were observed at stations: 57, 58, 62, 80, 81, 86, and 95 (Table 2), which often coincided with the lowest phosphate concentrations (Olofsson and Wulff, 2021). Chl-specific productivity ranged between <0.001 and 1.77 h⁻¹ (Fig. 2) with the highest values in stations dominated by haptophytes (Table S3), mainly *Phaeocystis* sp. (Olofsson and Wulff, 2021), and increasing towards the end of the cruise. The overall highest rate was observed in an ice-covered station (Fig. 2). The converted carbon-specific productivity ranged between <0.001 and 0.039 h⁻¹, and the growth rate based on carbon-doubling time was estimated in a range from <0.001 to 0.93 per day (Table 2). The fastest doubling times were often observed when both biomass and primary productivity was relatively high, dominating the stations further south (and later in the season).

3.2. Diurnal and depth integrated primary production

We used the measured primary productivity to estimate integrated rates based on light measurements at six stations. Results varied from 0.9 to 1382 mg C m $^{-2}$ d $^{-1}$ (Table 3). When we simulated rates at 0 and + 2 °C temperature, the elevated temperature provided the highest values while the *in situ* temperature was the lowest, suggesting a temperature limitation at the stations, which was dominated by temperatures below 0 °C (Table 1). However, there was no apparent difference in measured rates based on the temperature *in situ* (Tables 1 and 2).

3.3. UVBR effects on primary productivity

For the primary productivity we also addressed the effects of reduced UVBR on the incubations. There were no consistent effects on the primary productivity normalized to chl a (Fig. 2). This was further explored by comparing the relative primary productivity with and without UVBR (Fig. 3) where there was no consistent change; neither at surface nor in samples from deeper locations, and variation between replicates was large (demonstrated as standard deviation). Notably, the increase in primary productivity in the absence of UVBR was predominantly found at ice-covered stations (Fig. 3).

3.4. Photosynthetic pigments

The pigment concentrations varied a lot between stations (Fig. 4A) but with a more even relative contribution of each pigment (Fig. 4B). We did not observe a clear pattern between ice-covered and open water stations; of the twelve highest concentrations five were measured in icecovered stations (Tables 1 and S1). Carotenoids typical for specific microalgal groups showed overall weak correlations with cell numbers for the respective group (see below, and for detailed community composition see Olofsson and Wulff, 2021). The xanthophyll pigment 19-hex is a major pigment in the haptophyte Phaeocystis sp. (Zapata et al., 2004), and this genus also contains e.g., chl c3 and 19-but, however, the correlation between Phaeocystis sp. and 19-hex was quite weak (surface r = 0.40, $R^2 = 0.16$; deep r = 0.53, $R^2 = 0.28$). For chl c3, the correlation between haptophytes as a group as well as *Phaeocystis* sp. and chl c3 was moderate to strong (r = 0.80, $R^2 = 0.65$; r = 0.73, $R^2 =$ 0.54) but only for surface samples. However, 19-hex generally followed the increase in chl c3 (r = 0.69, $R^2 = 0.48$, n = 95). Fucox is a major pigment in diatoms but is also present in many other algal groups, e.g., chrysophytes, haptophytes, raphidophytes and some dinoflagellates (Jeffrey et al., 2011). Here, higher concentrations of fucox and diadin coincided with diatom cell numbers and equal correlation values for both surface and depth (fucox r = 0.82, $R^2 = 0.67$; diadin r = 0.81, $R^2 =$ 0.66). Diatox differed with the highest correlation values found for surface samples (r = 0.94, $R^2 = 0.88$), however, at several stations no diatox was detected. Perid did not corroborate the abundance of dinoflagellates but dinoflagellates are a complicated group with very different endosymbionts and not all dinoflagellates contain perid (Jeffrey et al., 2011). Prasin, present in the most abundant prasinophyte, Micromonas sp. showed overall a poor match between cell numbers and prasin concentrations. Chl b correlated well with violax (r = 0.69, $R^2 =$ 0.47, n = 110), both pigments present in chlorophytes and chrysophytes. Chrysophytes were rarely encountered except for station 48 (surface) and the deeper site at station 57. Violax and chl b showed weak correlations with cell numbers of autotrophic flagellates and prasinophytes. Allox is a specific marker pigment for cryptophytes and commonly found in the ciliate Mesodinium rubrum (with a cryptophycean symbiont) (Jeffrey et al., 2011). A weak correlation was observed for allox and cryptophytes, and a medium to weak positive correlation for Mesodinium rubrum (surface r = 0.54, $R^2 = 0.29$; deep r = 0.44, $R^2 = 0.19$).

The pigment ratios (diadin+diatox)/chl a, (violax+zeax)/chl a, and total carotenoids/chl a (Table S2) could be expected to increase with high radiation conditions. Here, these ratios did not significantly differ between surface and deep samples or between samples from ice-covered or open-water stations. Statistical tests and regression analyses indicated that depth alone or ice cover were not key determinants of these pigment ratios.

3.5. Mycosporine-like amino acids (MAAs)

Mycosporine-like amino acids (MAAs) concentrations, in relative absorbance units, varied between stations, where values above 6*10⁵ were observed at stations: 95, 58, 82, 81, 86, 80, 57, 62, 33, and 79, both surface and deep (Table S2). There was a strong correlation between MAAs, chl a and b-car2, respectively (r = 0.90, $R^2 = 0.82$; r = 0.84, $R^2 =$ 0.71, n = 91), however, the overall strongest correlation was found for chl c3 (r = 0.93, R² = 0.87, n = 91). Chl c3 is found in prymnesiophytes, some diatoms and the picoplanktonic bolidophytes (Jeffrey et al., 2011). The prymnesiophyte genus, Phaeocystis sp. is well-known to produce MAAs (Moisan and Mitchell, 2001). The pigments 19-hex and 19-but are also present in Phaeocystis sp. but showed a moderate and weak correlation to MAAs, respectively (r = 0.57, $R^2 = 0.32$; r = 0.30, $R^2 = 0.09$, n= 91). Fucox, also present in *Phaeocystis* sp., showed a strong positive correlation with MAAs (r = 0.78, $R^2 = 0.61$, n = 91). Fucox is the major xanthophyll in diatoms but is also present in e.g. Phaeocystis sp. Other photosynthetic pigments with strong positive correlation to MAAs were chl c1c2 (r = 0.83, R² 0.69, n = 91), diadin (r = 0.74, R² = 0.54, n = 91), and prasin (r = 0.73, $R^2 = 0.53$, n = 91).

Table 2 Primary productivity, chl a concentration (mean \pm SD), chl a-specific productivity, carbon concentration converted from chl a, C-specific C-productivity, carbon-doubling time, growth rate (d⁻¹), and PAR in air at measuring time (UTC), from surface samples with UVBR.

St.	Primary productivity ($\mu g \ C \ l^{-1} \ h^{-1}$)	Rough daily productivity (mg C m $^{-2}$ d $^{-1}$)	Chl a $(\mu g l^{-1})$	Chl-specific productivity (C Chl^{-1} h^{-1})	Carbon (μg l ⁻¹)	C-specific C-prod h ⁻¹	C-doubling time (days)	Growth rate (d ⁻¹)	PAR (μ mol photons m ⁻² s ⁻¹)
10	0.193	46.3	1.02 ±	0.189	41	0.005	8.82	0.11	400 (10:00)
14	0.014	3.4	$0.18 \\ 0.12 \pm \\ 0.02$	0.118	5	0.003	14.08	0.07	500 (14:00)
8	no PP	no PP	0.11	no PP	4	no PP	no PP	no PP	370 (12:30)
20	0.002	0.5	0.10 ± 0.03	0.021	4	0.001	80.19	0.01	450 (12:30)
1	0.001	0.1	0.13 ± 0.02	0.004	5	< 0.001	>100	< 0.01	435 (14:45)
23	0.015	3.6	$\begin{array}{c} 0.10 \; \pm \\ 0.01 \end{array}$	0.152	4	0.004	11.00	0.09	470 (11:15)
5	0.014	3.4	$\begin{array}{c} 0.09 \pm \\ 0.02 \end{array}$	0.157	4	0.004	10.59	0.09	460 (12:30)
3	na	na	$\begin{array}{c} 1.43 \pm \\ 0.12 \end{array}$	na	57	na	na	na	660 (12:50)
6	0.063	15.2	0.12 ± 0.02	0.528	5	0.013	3.16	0.32	720 (13:05)
8	0.065	15.6	0.17 ± 0.00	0.383	4	0.015	2.81	0.36	-
10	0.049	11.7	0.19 ± 0.01	0.256	8	0.006	6.51	0.15	670 (12:20)
1	no PP	no PP	0.12 ± 0.01	no PP	5	no PP	no PP	no PP	-
4	0.001	0.3	1.36 ± 0.29	0.001	54	< 0.001	>100	< 0.01	505 (12:15)
5	0.001	0.1	0.29 0.97 ± 0.03	0.001	39	< 0.001	>100	< 0.01	-
8	0.001	0.2	0.48 ± 0.03	0.001	19	< 0.001	>100	< 0.01	920 (12:30)
9	0.055	13.1	0.36 ± 0.04	0.152	14	0.004	10.96	0.09	-
4	0.047	11.3	0.04 0.48 ± 0.09	0.098	19	0.002	17.02	0.06	950 (12:50)
5	0.001	0.3	0.41 ± 0.05	0.003	16	< 0.001	>100	< 0.01	-
7	na	na	6.92 ± 2.87	na	268	na	na	na	303 (15:40)
8	6.888	1653.2	10.39 ± 1.57	0.663	416	0.017	2.51	0.40	-
2	3.126	750.4	6.44 ± 0.29	0.485	258	0.012	3.43	0.29	750 (09:00)
9	no PP	no PP	0.29 0.31 ± 0.01	no PP	12	no PP	no PP	no PP	-
0	0.056	13.5	$0.01 \\ 0.22 \pm \\ 0.07$	0.255	6	0.010	4.15	0.24	360 (09:00)
1	0.067	16.2	0.07 0.27 ± 0.09	0.250	11	0.006	6.67	0.15	-
' 4	_	-	0.05 0.15 ± 0.03	-	-	-	-	-	850 (12:30)
5	no PP	no PP	0.05 0.15 ± 0.00	no PP	6	no PP	no PP	no PP	-
7	no PP	no PP	0.39 ± 0.08	no PP	18	no PP	no PP	no PP	-
0	4.666	1119.8	5.65 ± 1.94	0.826	226	0.021	2.02	0.50	270 (12:45)
1	3.863	927.2	3.10 ± 0.55	1.246	99	0.039	1.07	0.93	-
3	0.139	33.3	0.57 ± 0.16	0.244	23	0.006	6.84	0.15	287 (13:35)
6	4.389	1053.3	3.87 \pm	1.134	155	0.028	1.47	0.68	-
8	no PP	no PP	0.52 0.21 ±	no PP	5	no PP	no PP	no PP	-
9	0.206	49.5	(na) 0.60 ±	0.344	24	0.009	4.85	0.21	142 (12:15)
1	0.206	49.4	0.04 0.65 ±	0.317	26	0.008	5.26	0.19	_
5	11.664	2799.3	0.22 9.87 ±	1.182	395	0.030	1.41	0.71	740 (12:45)
6	0.395	94.8	$\begin{array}{l} 0.23 \\ 0.33 \ \pm \end{array}$	0.197	13	0.030	1.39	0.72	_

na = error with the measurements. No primary productivity (no PP) equals when dark production exceeds light production.

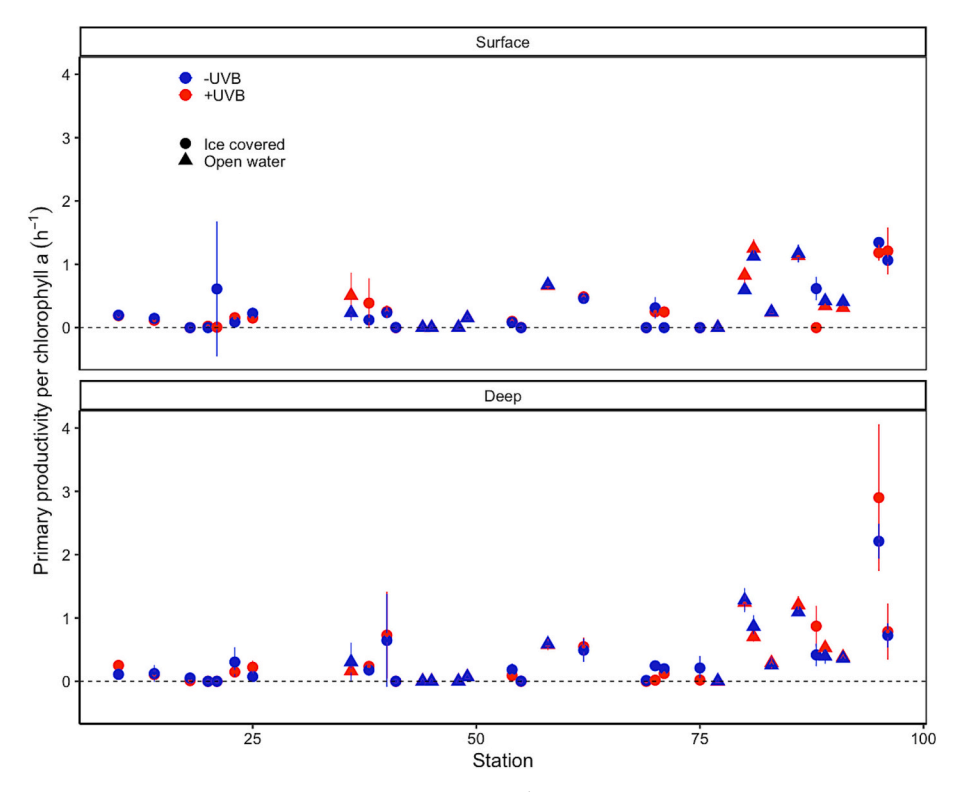


Fig. 2. Primary productivity normalized to chlorophyll a concentration (μg C μg chl a^{-1}) for each station with and without UVBR at either surface (upper panel) or deep (lower panel). Symbols indicate if water was sampled under ice or in open water. n = 3, error bars show standard deviation.

Table 3 Modeled integrated production (mg C m $^{-2}$ d $^{-1}$ at *in situ* temperature, at 0, and at +2 °C), C doubling time at 2.5 m (similar to sampling depth) from the model, and roughly estimated integrated production (assuming 24 h of light and activity to 10 m depth) from incubation experiments, and measured chl a concentration (µg l $^{-1}$). For ice conditions during sampling see Table 1.

Station	14	20	23	25	40	58
Date	May 2, 2002	May 4, 2022	May 7, 2022	May 10, 2022	May 14, 2022	May 19, 2022
In situ temp	6.83	0.87	4.39	5.39	16.9	1382.0
0 °C	7.65	0.97	4.92	6.01	18.9	1392.7
+2 °C	8.68	1.10	5.58	6.82	21.4	1579.8
C doubling time 2.5 m depth, d	16.7	105.7	14.1	13.8	9.12	3.94
Rough estimate	3.4	0.5	3.6	3.4	11.7	1653.2
Chl a	0.122	0.096	0.097	0.093	0.192	10.38

When normalizing MAAs to chl a, there was no consistent pattern indicating that ice-covered stations had lower values compared to openwater stations (Fig. 5). High ratios were generally observed at stations with haptophytes and low values with diatoms (Fig. 5; Tables S2 and S3). The overall highest MAAs chl $\rm a^{-1}$ ratio was observed at station 14, dominated by haptophytes, which was also close to neutral in response to UVBR (Fig. 3), suggesting that haptophytes could be best prepared for variable UVBR. However, MAAs chl $\rm a^{-1}$ had a unimodal relationship with light intensity across the stations (Fig. S3) where the highest ratios were observed at stations with intermediate light intensities in the surface waters.

4. Discussion

The Arctic ecosystem is in the midst of major climate-related changes including elevated temperatures, with sea ice retreat as a direct

consequence. This leads to restructuring of phytoplankton communities, affecting seasonality and overall increased primary production in the Arctic (Arrigo and van Dijken, 2015; Renaut et al., 2018; Lebrun et al., 2019). The cruise data presented here (EGC, May 2002) demonstrated large variation along the transects with patchiness and locally high primary productivity rates. The highest primary productivity normalized to chl a was observed at stations with haptophytes, typically dominated by Phaeocystis sp. The pattern is in concert to studies from Antarctica, with relatively higher production rates as compared to diatom dominated communities (Smith Jr. et al., 2021). We previously published data from the same cruise as herein, covering the microplanktonic biodiversity and community composition (Olofsson and Wulff, 2021), with no correlation between high diversity and high primary productivity, a topic under continuous debate (Pillai and Gouhier, 2019; Vallina et al., 2014). Our data, thus, support the theory of a nonlinear relationship between the two (Vallina et al., 2014). On the other hand, other factors can be equally important to the stability of the ecosystem, such as grazing, hydrographic conditions affecting the mixed layer depth, temperature, and nutrient availability, and seasonality can all affect food transfer to higher trophic levels (Renaud et al., 2024) and biogeochemical cycles (Thomalla et al., 2023).

We investigated how primary productivity rates were affected by UVBR exposure during the incubation experiment. No statistically significant effect was detected, and the organisms exhibited no evidence of adverse responses to UVBR exposure. Notably, some of the highest levels of enhanced primary productivity in the absence of UVBR were observed at ice-covered stations, suggesting that microalgal communities in these environments were adapted to low-light conditions with UV radiation protection mechanisms that were inactive or not induced. It is well established that low-light acclimation increases sensitivity to UV radiation, as already demonstrated by Helbling et al. (1992). However, in our experiment, no clear differences in UVBR sensitivity were observed between communities sampled from under ice and those from open water stations. It should be noted that UVBR intensities were not matched to the comparatively lower PAR levels, which could have led to

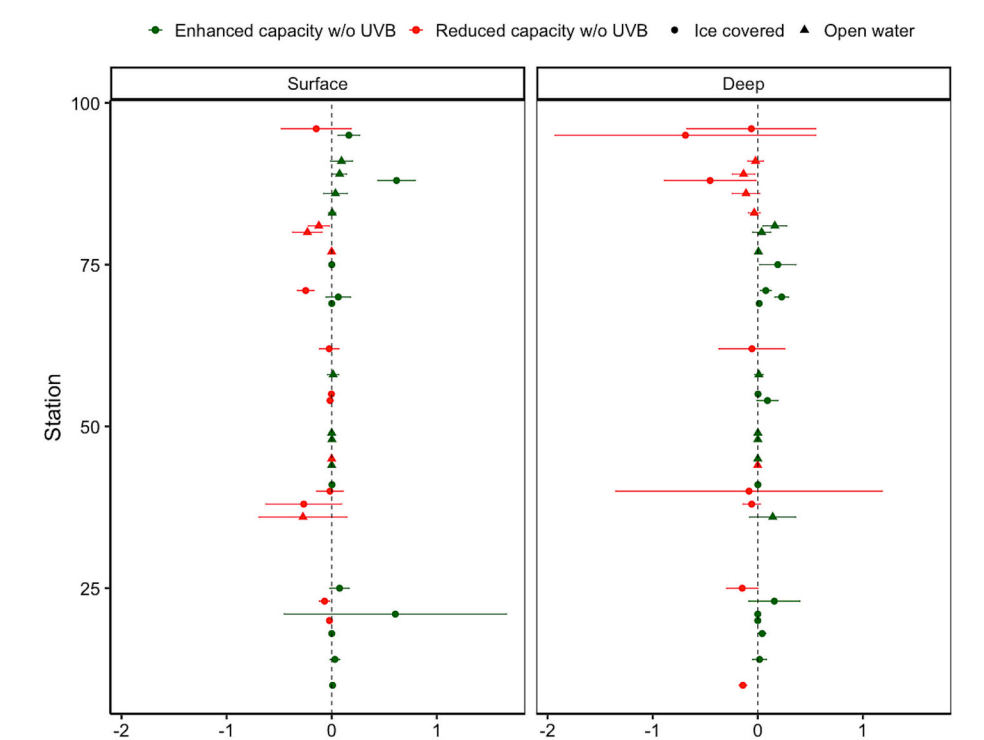


Fig. 3. Difference in primary productivity per chl a in the UVBR exposure experiment. Green dots indicate enhanced capacity when incubated in -UVBR as compared to +UVBR, and reduced capacity means when incubated with UVBR resulted in higher primary productivity per chl a as compared to without UVBR. Surface samples are shown in the left panel and deep samples in the right panel. Symbols indicate if water was sampled under ice or in open water. n = 3, error bars show standard deviation. (For interpretation of the references to colour in this figure legend, the reader is referred to the web version of this article.)

Difference

an overestimation of potential UVBR effects. Additionally, no supplementary UVAR was included, but since no adverse effects were observed, this potential bias does not appear to have influenced the results. The concentration of photosynthetic pigments and MAAs varied largely between stations, as also the abundance and composition of phytoplankton. However, the relative pigment composition was fairly similar among stations despite the large difference in the total pigment concentrations. Further, in general, high MAAs chl a⁻¹ was observed at stations with haptophytes and, moreover, a strong positive correlation was found for chl c3 and MAAs. Stations with high numbers of diatoms showed low MAAs chl a⁻¹ ratios despite the strong correlation between MAAs and fucox, the major xanthophyll in diatoms. This is in concert with Ha et al. (2012) from Kongsfjorden, Svalbard, where high MAAs chl a⁻¹ ratios were observed for *Phaeocystis* sp. while the opposite for the diatom Thalassiosira sp. both dominating the spring bloom. Weiss et al. (2022) found a strong correlation between haptophytes and the diversity of MAAs in the Southern Ocean, and the highest ratios of MAAs chl a⁻¹ were associated with the haptophyte population. Interestingly, as observed by Riegger and Robinson (1997), MAAs in Phaeocystis antarctica were mostly found within the extracellular colonial matrix. In our study, we were not able to make such a distinction. Underwater radiation measurements at four o'clock in the afternoon on three occasions in May averaged between 98 and 23 μ mol photons m⁻² s⁻¹ (PAR) at depths ranging from 1.5 m to 21 m. Neither the radiation intensities nor the depth differences were likely large enough to induce the accumulation or production of MAAs. Therefore, the MAAs concentrations were most likely due to the community composition rather than the radiation intensities per se. Further supporting this conclusion, the pigment ratios (diadin+diatox) chl a⁻¹, (violax+zeax) chl a⁻¹, and total carotenoids chl a⁻¹ did not significantly differ between surface and deep samples or between ice-covered or open water stations.

To estimate depth integrated diurnal production, we used two different approaches. First, we roughly estimated the integrated

production assuming that the production measured from the surface sample was representative for the upper 10 m and that light was available for 24 h (midnight sun). Secondly, we applied a model based on the measured primary productivity and measured light profiles, and calculated light intensities at each hour and by each depth, based on Pabi et al. (2008), to estimate the size of the production over time using our production rate measurement as input. Even though the two approaches differ substantially in complexity they gave qualitatively similar estimates looking at ranking. The modelling approach gave 10–90 % higher estimates, except at station 58 where the rough estimate gave a 25 % higher value. This was the overall highest production and the only of the modeled ones that was based on production measurements from samples collected in open water. This suggests that the rough estimate underestimates the production and the values in Table 2 are potentially higher in reality, but they provide a hint of the order of magnitude for primary production for the region during early spring conditions.

Until recently, under-ice primary productivity has been underestimated due to the assumption of low light intensities. This has likely led to underestimations of total primary production in the Arctic and introduced biases in projections of climate change impacts. However, consistent with our findings, previous studies have reported massive phytoplankton blooms under sea ice, with productivity levels in early spring sometimes exceeding those in open waters (Arrigo et al., 2012, 2014; Arrigo and van Dijken, 2015). For example, in our study the second highest chl a concentration and the highest primary productivity were recorded at an under-ice station (Tables 1 and 2). Despite this, we found no significant correlation between ice cover and primary productivity. A potential limitation is that incubations were carried out under uniform light conditions onboard the vessel, possibly reducing the influence of actual light differences between ice-covered and open-water sites. Nevertheless, our data point to a high productivity potential in iceassociated Phaeocystis populations, consistent with observations from late May at an ice-covered station north of Svalbard (Assmy et al., 2017).

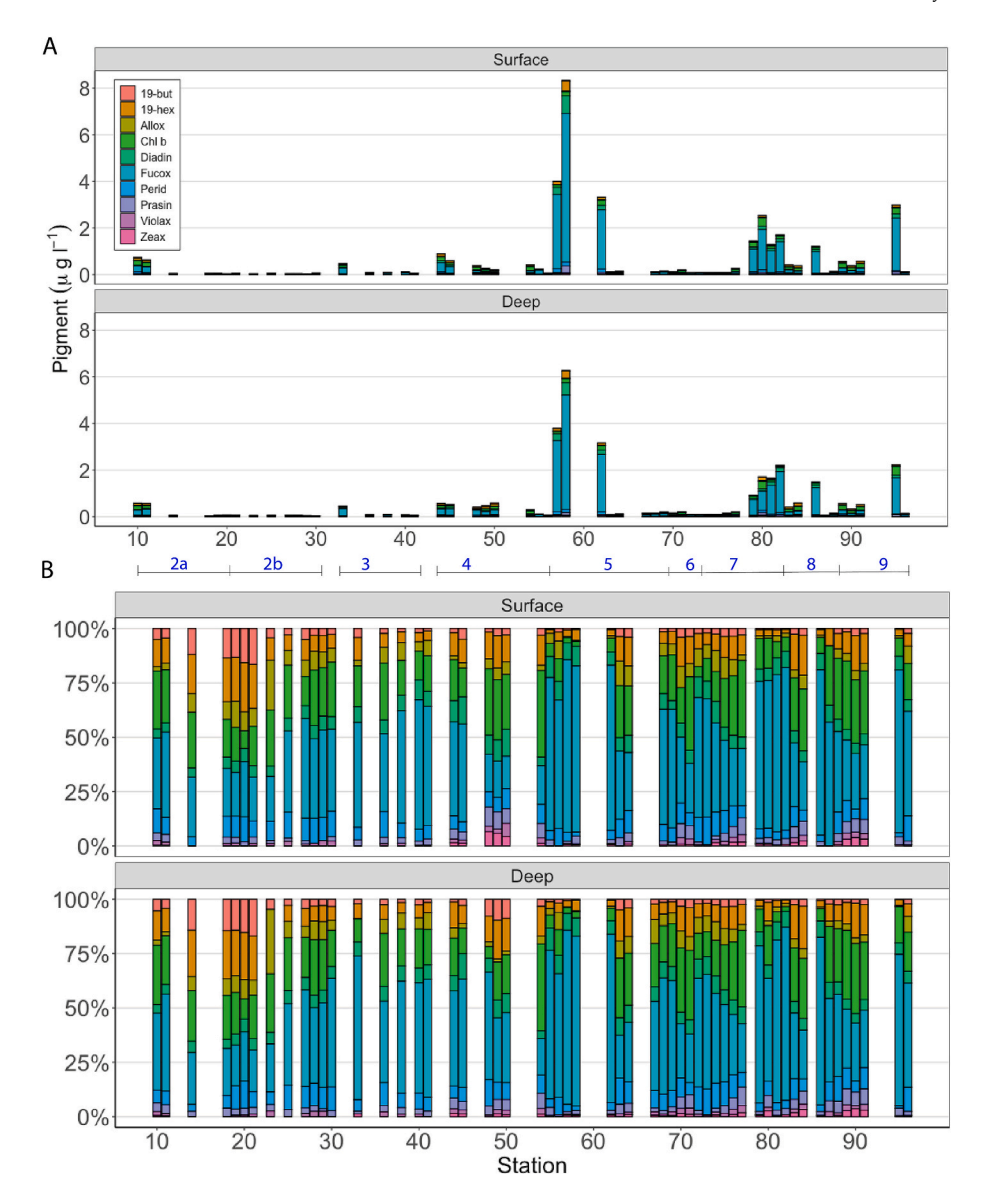


Fig. 4. A) Pigment concentrations as μ g l⁻¹ and, B) their relative concentration for each station in surface and deep samples. Transect numbers are included in dark blue with horizontal bars indicating the stations. (For interpretation of the references to colour in this figure legend, the reader is referred to the web version of this article.)

Given the substantial reduction in ice cover in this region since our sampling two decades ago (King et al., 2020), our dataset provides a valuable historical baseline for evaluating ongoing and future changes in Arctic primary productivity.

The field survey was conducted during an early bloom situation, as indicated by occasionally high biomass and still fairly high concentrations of inorganic nutrients (Olofsson and Wulff, 2021). Some stations had already developed bloom situations, for example stations 80-82, and 95, visited later in May and located further south. This temporal pattern was also observed in the bloom set-off in Svalbard (Assmy et al., 2017). The highest model-based integrated primary productivity rates was observed at station 58 with rates of 1382 mg C m⁻² d⁻¹, which is above that of temperate areas (Swedish west coast) under spring bloom conditions of \sim 250–500 mg C m⁻² d⁻¹ (Tiselius et al., 2015) and the Canadian High Arctic during late summer and fall spanning from 49 to 448 mg C m⁻² d⁻¹ (Ardyna et al., 2011). However, Richardson et al. (2005) measured primary productivity in the Greenland sea as ranging from 0.40 to 2400 mg C m⁻² d⁻¹ with the highest production in late May and June, and Matrai et al. (2013) synthesised available rates in the Arctic over 50 years with an average in spring of 108 mg m-3 d^{-1} , which

is in the higher range of our estimates, assuming 10 m depth of production as herein. A majority of the stations had much lower rates, with a mean of 225 mg C m⁻² d⁻¹. Ardyna et al. (2011) observed the highest primary productivity in Baffin Bay at 75° to 80° N, under nutrient replete conditions in a phytoplankton community dominated by large diatoms, e.g., Chaetoceros spp. and temperature of 0.6 °C, but rates were > 300 mg C m $^{-2}$ d $^{-1}$ also at -0.3 and - 0.9 °C. In a study based on estimates from satellite images, spring bloom primary productivity was estimated to range between 500 and 1000 mg C m⁻² d⁻¹ (Renaut et al., 2018), and chl a values between 0.8 and 6.5 $\mu g \, l^{-1}$, which is comparable to our observations as well. Satellite estimates are useful and cover large spatial and temporal scales, but they need to be validated to in situ measurements. The substantial variation in rates reflects a combination of natural spatial heterogeneity and methodological differences, both of which influence the observed outcomes. Further, many recent studies use satellite imaging to estimate primary productivity (Arrigo and van Dijken, 2015; Renaut et al., 2018), challenging the comparison of data sets and changes across the last two decades. This spring bloom primary production is the basis of the Arctic food web and is therefore of importance to study for projecting future situations in timing,

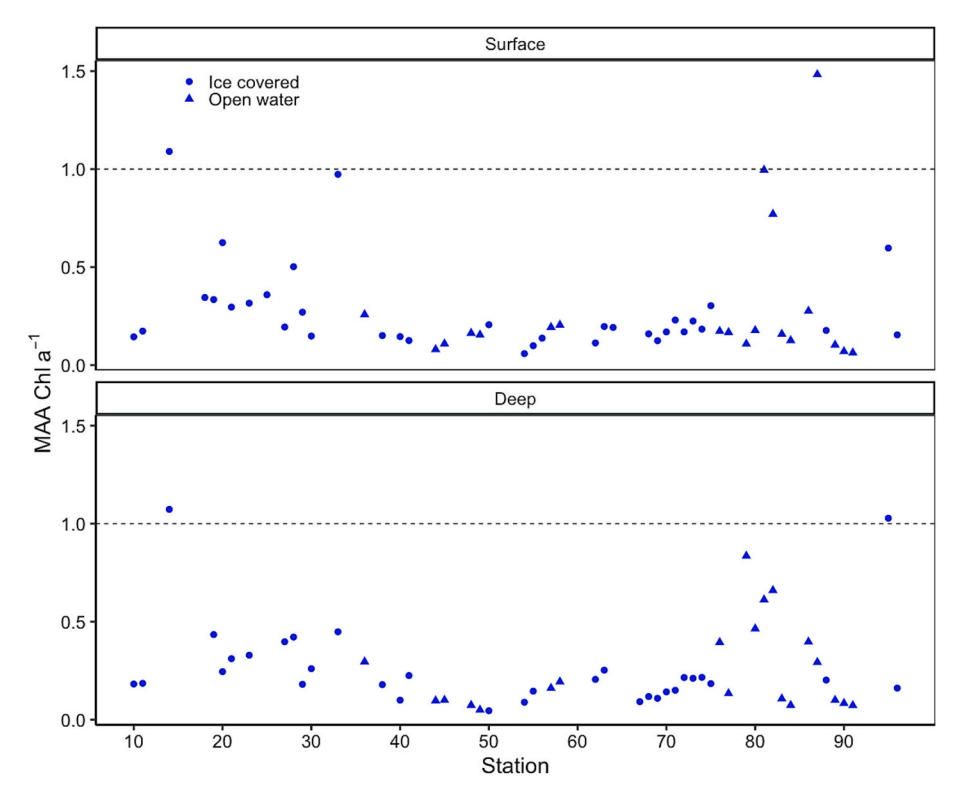


Fig. 5. Mycosporine-like amino acids (MAAs) concentration (absorbance l^{-1}) per chlorophyll a concentration (absorbance l^{-1}), presented as MAAs chl a^{-1} . Symbols indicate if water was sampled under ice or in open water. Dashed lines indicate the 1:1 ratio.

magnitude, and community composition.

The sampled upper water mass herein was well mixed when comparing temperatures, salinities, and inorganic nutrients between surface and deep samplings (Table 1 and nutrients in Olofsson and Wulff, 2021). A similar composition of phytoplankton communities was also observed between sampling depths. Nutrients were never depleted, with the lowest concentration at stations with the highest chl a concentration, as station 95, where also carbon-doubling rates were up to almost 1 day, only, which is equal to diatoms during exponential growth phase under laboratory conditions (Olofsson et al., 2019). High growth rates were recently also quantified in populations of the ice algae *Ancylonema* sp. with doubling times of less than 2 days (Halbach et al., 2025). However, potential carbon doubling times were often much slower with some stations with doubling times above 100 days (Table 2), where potential rates are used as they were quantified under saturated light conditions.

As mentioned, productivity and diversity measurements were not correlated in the present study. The species diversity was generally lower at stations where only one or a few species/genera dominated, e. g., Phaeocystis sp. with for example an effective species number of 1.67 (station 95), but with high primary productivity of 11.6 μ g C l⁻¹ h⁻¹ and carbon-doubling times of 1.4 days. Chl a was measured in bulk samples and can therefore not be converted to carbon on species level but rather using an average for all species within each sample. Since diatoms are known to have about 1.5-2.5 times higher chl a to carbon ratios as compared to haptophytes, the average ratio used for both groups potentially overestimate the carbon concentration of haptophytes while overestimating carbon-doubling times. Therefore, at stations dominated by haptophytes, real carbon-doubling times were potentially even faster, although the maximum growth rates were still high for natural bloom conditions even in temperate waters (Sakshaug et al., 2009). The chlorophyll specific productivity on station 95 (haptophyte dominated) and 62 (diatom dominated) were 1.19 d⁻¹ and 0.49 d⁻¹, respectively, resulting in also slower growth rates for the diatoms, with 0.71 d⁻¹ and $0.29 \,\mathrm{d^{-1}}$, respectively. Maximum growth rates at $-0.5\,^{\circ}\mathrm{C}$ for the region

for diatoms are about $0.5 d^{-1}$ (Sakshaug et al., 2009), so this was below, but can potentially include a partly inactive carbon biomass.

The incubation experiments were conducted at constant temperature (controlled water baths), and therefore did not reflect the natural variation in in situ temperatures of the natural communities. If sampled communities were locally adapted to temperature in terms of photosynthetic pigment or protein composition, differences in primary productivity would be expected. We, however, observed high primary productivity rates both in relation to chl a and per liter, both in communities collected from stations with low (station 95 with -1.7 °C) and relatively higher temperatures (station 58 with 3.5 °C). The benefit here of using the model was that we could run it with also higher temperatures, where higher primary productivity was always observed with higher temperatures. Responses to temperature changes are usually expressed as Q10-value. Q10 values for primary productivity generally differ substantially (Bindoff et al., 2019) and are often not quantified at temperatures realistic for the Arctic Ocean (-2 °C - +2 °C). As also discussed in Laufkötter et al. (2015) this estimate varies significantly between investigations and can also vary depending on species. Further, the basic relationship between changed temperature and primary productivity is based on Eppley (1972), where data comes from investigations using cultures grown at different temperatures (between 2 and 40 °C) at continuous light. Eppley (1972) comments that the Q10value following this equation is lower than what to expect from photosynthesis measurements in natural waters. With the importance of changes in production following temperature increase, as we demonstrate with the model (see Table 2), there is a need for a revisit of the Q10 value for phytoplankton production in cold waters when estimating primary productivity for this region, as temperatures below 2 °C are not included in the relationship by Eppley (1972) and modern methods might be applied for more accurate estimates.

Further understanding of potential effects of climate change and ice decline is fundamental for the primary producers of the future Arctic. This data set provides an insight into primary productivity rates 20+ years ago, which enables comparisons to recent measurements, to clarify

how the communities are affected by increased temperatures and less sea ice. Primary productivity is the basis of all life and with changes in temperature and nutrient cycling along with climate change, we can expect revision also at higher trophic levels.

CRediT authorship contribution statement

Malin Olofsson: Writing – review & editing, Writing – original draft, Visualization, Validation, Formal analysis, Data curation. Sten-Åke Wängberg: Writing – review & editing, Methodology, Investigation, Conceptualization. Anna Engelsen: Writing – review & editing, Validation, Methodology, Investigation, Formal analysis, Data curation. Angela Wulff: Writing – review & editing, Writing – original draft, Validation, Supervision, Resources, Project administration, Methodology, Investigation, Funding acquisition, Formal analysis, Data curation, Conceptualization.

Declaration of competing interest

The authors declare that they have no known competing financial interests or personal relationships that could have appeared to influence the work reported in this paper.

Acknowledgements

We thank the captain and crew of I/B Oden for their assistance during the cruise, everybody running the rosette sampler and performing on-board analyses of e.g. salinity and temperature. A special thanks to S. Becker, UCSD/SIO Oceanographic Data Facility for the nutrient data. M. Appelgren is acknowledged for assistance with HPLC analyses. This research has been supported by grants from the Swedish Polar Research Secretariat, the YMER-80 Foundation, the Lennander Foundation, the Lars Hierta Memorial Foundation, and Wilhelm and Martina Lundgren's Science Fund.

Appendix A. Supplementary data

Supplementary data to this article can be found online at https://doi.org/10.1016/j.seares.2025.102608.

Data availability

Data will be made available on request.

References

- Ærtebjerg Nielsen, G., Bresta, A., 1984. Guidelines for the measurements of phytoplankton primary production. Balt. Mar. Biol. 1, 1–23.
- Ardyna, M., Gosselin, M., Michel, C., Poulin, M., Tremblay, J.E., 2011. Environmental forcing of phytoplankton community structure and function in the Canadian High Arctic: contrasting oligotrophic and eutrophic regions. Mar. Ecol. Prog. Ser. 442, 37–57. https://doi.org/10.3354/meps09378.
- Arrigo, K.R., van Dijken, G.L., 2015. Continued increases in Arctic Ocean primary production. Prog. Oceanogr. 136, 60–70. https://doi.org/10.1016/j. pocean.2015.05.002.
- Arrigo, K.R., Worthen, D., Schnell, A., Lizotte, M.P., 1998. Primary production in Southern Ocean waters. J. Geophys. Res. 103 (C8), 587–600. https://doi.org/ 10.1029/98JC00930, 15.
- Arrigo, K.R., van Dijken, G.L., Bushinsky, S., 2008. Primary production in the Southern Ocean 1997–2006. J. Geophys. Res. 113, C08004. https://doi.org/10.1029/ 2007.IC004551.
- Arrigo, K.R., Perovich, D.K., Pickart, R.S., Brown, Z.W., van Dijken, G.L., Lowry, K.E., et al., 2012. Massive phytoplankton blooms under Arctic sea ice. Science 336. https://doi.org/10.1126/science.1215065, 1408-1408.
- Arrigo, K.R., Perovich, D.K., Pickart, R.S., Brown, Z.W., van Dijken, G.L., Lowry, K.E., et al., 2014. Phytoplankton blooms beneath the sea ice in the Chukchi Sea. Deep-Sea Res. II 105, 1–16. https://doi.org/10.1016/j.dsr2.2014.03.018.
- Assmy, P., Fernández-Méndez, M., Duarte, P., Meyer, A., Randelhoff, A., Mundy, C.J., et al., 2017. Leads in Arctic pack ice enable early phytoplankton blooms below snow-covered sea ice. Sci. Rep. 7, 40850. https://doi.org/10.1038/srep40850.
- Bindoff, N.L., et al., 2019. Changing ocean, marine ecosystems, and dependent communities. In: Pörtner, H.-O., Roberts, D.C., Masson-Delmotte, V., Zhai, P.,

- Tignor, M., Poloczanska, E., Mintenbeck, K., Alegría, A., Nicolai, M., Okem, A., Petzold, J., Rama, B., Weyer, N.M. (Eds.), IPCC Special Report on the Ocean and Cryosphere in a Changing Climate. Cambridge University Press, Cambridge, UK and New York, NY, USA, pp. 447–587. https://doi.org/10.1017/9781009157964.007.
- Bouchard, J.N., Roy, S., Ferreyra, G., Campbell, D.A., Curtosi, A., 2005. Ultraviolet-B effects on photosystem II efficiency of natural phytoplankton communities from Antarctic. Polar Biol. 28, 607–618. https://doi.org/10.1007/s00300-005-0727-4.
- Campbell, G.S., Norman, J.M., 1998. An Introduction to Environmental Biophysics, 2nd edition. Springer Book Archive. https://doi.org/10.1007/978-1-4612-1626-1. 978-0-387-94937-6.
- Carreto, J.I., Carignan, M.O., Montoya, N.G., 2005. A high-resolution reverse-phase liquid chromatography method for the analysis of mycosporin-like amino-acids (MAAs) in marine organisms. Mar. Biol. 146, 237–252. https://doi.org/10.1007/ s00227-004-1447-y.
- Castellani, G., Veyssière, G., Karcher, M., Stroeve, J., Banas, S.N., Bouman, A.H., Brierley, S.A., et al., 2022. Shine a light: under-ice light and its ecological implications in a changing Arctic Ocean. Ambio 51 (2), 307–317. https://doi.org/10.1007/s13280-021-01662-3.
- Eppley, R.W., 1972. Temperature and phytoplankton growth in the sea. Fish. Bull. 70 (4),
- Ha, S.-Y., Kim, Y.N., Park, M.O., Kang, S.H., Kim, H.C., Shin, K.H., 2012. Production of mycosporine-like amino acids of in situ phytoplankton community in Kongsfjorden, Svalbard, Arctic. J. Photochem. Photobiol. B Biol. 114 (3), 1–14. https://doi.org/ 10.1016/j.jphotobiol.2012.03.011.
- Halbach, L., Kitzinger, K., Hansen, M., Littmann, S., Benning, L.G., Bradley, J.A., et al., 2025. Single-cell imaging reveals efficient nutrient uptake and growth of microalgae darkening the Greenland ice sheet. Nat. Commun. 16, 1–14. https://doi.org/ 10.1038/s41467-025-56664-6.
- Helbling, E.W., Villafañe, V., Ferrario, M., Holm-Hansen, O., 1992. Impact of natural ultraviolet radiation on rates of photosynthesis and on specific marine phytoplankton species. Mar. Ecol. Prog. Ser. 80 (1), 89–100.
- IPCC, 2023. Summary for policymakers. In: Core Writing Team, Lee, H., Romero, J. (Eds.), Climate Change 2023: Synthesis Report. Contribution of Working Groups I, II and III to the Sixth Assessment Report of the Intergovernmental Panel on Climate Change. IPCC, Geneva, Switzerland, pp. 1–34. https://doi.org/10.59327/IPCC/AR6-9789291691647.001.
- Jeffrey, S.W., Wright, S.W., Zapata, M., 2011. Microalgal classes and their signature pigments. In: Roy, S., Llewellyn, C.A., Egeland, E.S., Johnsen, G. (Eds.), Phytoplankton Pigments: Characterization, Chemotaxonomy and Applications in Oceanography. Cambridge University Press, pp. 3–77. United Kingdom. (ISBN 9780511732963)
- King, M.D., Howat, I.M., Candela, S.G., et al., 2020. Dynamic ice loss from the Greenland ice sheet driven by sustained glacier retreat. Commun. Earth Environ. 1, 1. https://doi.org/10.1038/s43247-020-0001-2.
- Laufkötter, C., Vogt, M., Gruber, N., Aita-Noguchi, M., Aumont, O., Bopp, L., Buitenhuis, E., et al., 2015. Drivers and uncertainties of future global marine primary production in marine ecosystem models. Biogeosciences 12, 6955–6984. https://doi. org/10.5194/bg-12-6955-2015.
- Lebrun, M., Vancoppenolle, M., Madec, G., Massonnet, F., 2019. Arctic sea-ice-free season projected to extend into autumn. Cryosphere 13, 79–96. https://doi.org/
- Leu, E., Graeve, M., Wulff, A., 2016. A (too) bright future? Arctic diatoms under radiation stress. Polar Biol. 39, 1711–1724. https://doi.org/10.1007/s00300-016-2003-1.
- Lund-Hansen, L.C., Hawes, I., Hancke, K., Salmansen, N., Nielsen, J.R., Balslev, L., Sorrell, B.K., 2020. Effects of increased irradiance on biomass, photobiology, nutritional quality, and pigment composition of Arctic sea ice algae. Mar. Ecol. Prog. Ser. 648, 95–110. https://doi.org/10.3354/meps13411.
- Manizza, M., Caroll, D., Menemenlis, D., Zhang, H., Miller, C.E., 2023. Modeling the recent changes of phytoplankton blooms dynamics in the Arctic Ocean. J. Geophys. Res. Oceans 6 (128), 1–22. https://doi.org/10.1029/2022JC019152.
- Matrai, P.A., Olson, E., Suttles, S., Hill, V., Codispoti, L.A., Light, B., Steele, M., 2013. Synthesis of primary production in the Arctic Ocean: I. Surface waters, 1954–2007. Prog. Oceanogr. 110, 93–106.
- Meredith, M., et al., 2019. Polar regions. In: Pörtner, H.-O. (Ed.), IPCC Special Report on the Ocean and Cryosphere in a Changing Climate. Cambridge University Press, Cambridge, UK and New York, NY, USA, pp. 203–320. https://doi.org/10.1017/ 9781009157964.001.
- Moisan, T.A., Mitchell, B.G., 2001. UV absorption by mycosporine-like amino acids in Phaeocystis antarctica Karsten induced by photosynthetically available radiation. Mar. Biol. 138, 217–227. https://doi.org/10.1007/s002270000424.
- Neale, P.J., Williamson, C.E., Banaszak, A.T., Häder, D.P., Hylander, S., Ossola, R., et al., 2023. The response of aquatic ecosystems to the interactive effects of stratospheric ozone depletion, UV radiation, and climate change. Photochem. Photobiol. Sci. 22, 1093–1127. https://doi.org/10.1007/s43630-023-00370-z.
- Nilsson, J., Björk, G., Rudels, B., Winsor, P., Torres, D., 2008. Liquid freshwater transport and polar surface water characteristics in the East Greenland current during the AO-02 oden expedition. Prog. Oceanogr. 78, 45–57. https://doi.org/10.1016/j. pocean 2007.06.002
- Olofsson, M., Wulff, A., 2021. Looking back to the future—micro- and nanoplankton diversity in the Greenland Sea. Mar. Biodivers. 51, 61. https://doi.org/10.1007/
- Olofsson, M., Kourtchenko, O., Zetsche, E.-M., Marchant, H.K., Whitehouse, M.J., Godhe, A., Ploug, H., 2019. High single-cell diversity in carbon and nitrogen assimilation by a chain-forming diatom across a century. Environ. Microbiol. 21 (1), 142–151. https://doi.org/10.1111/1462-2920.14434.

- Pabi, S., van Dijken, G.L., Arrigo, K.R., 2008. Primary production in the Arctic Ocean 1988-2006. J. Geophys. Res. 113. https://doi.org/10.1029/2007JC004578.
- Parsons, T.R., Maita, Y., Lalli, C.M., 1984. A Manual of Chemical and Biological Methods for Seawater Analysis, 1 ed. Pergamon Press, Oxford, England. ISBN: 0-08-030287-4
- Pillai, P., Gouhier, T.C., 2019. Not even wrong: the spurious measurement of biodiversity's effect on ecosystem functioning. Ecology 100 (7), 1–12. https://doi. org/10.1002/ecv.2645.
- Platt, T., Harrison, W.G., Irwin, B., Horne, E.P., Gallegos, C.L., 1982. Photosynthesis and photoadaptation of marine phytoplankton in the Arctic. Deep Sea Res. A: Oceanogr. Res. Pap. 29, 1159–1170. https://doi.org/10.1016/0198-0149(82)90087-5.
- Rantanen, M., Karpechko, A.Y., Lipponen, A., et al., 2022. The Arctic has warmed nearly four times faster than the globe since 1979. Commun. Earth Environ. 3, 168.
- Renaud, P.E., Daase, M., Leu, E., Geoffroy, M., Basedow, S., Inall, M., et al., 2024. Extreme mismatch between phytoplankton and grazers during Arctic spring blooms and consequences for the pelagic food-web. Prog. Oceanogr. 229, 103365. https:// doi.org/10.1016/j.pocean.2024.103365.
- Renaut, S., Devred, E., Babin, M., 2018. Northward expansion and intensification of phytoplankton growth during the early ice-free season in Arctic. Geophys. Res. Lett. 45. https://doi.org/10.1029/2018GL078995.
- Richardson, K., Markager, S., Buchc, E., Lassen, M.F., Kristensen, S., 2005. Seasonal distribution of primary production, phytoplankton biomass and size distribution in the Greenland Sea. Deep-Sea Res. I 52 (2005), 979–999.
- Riegger, L., Robinson, D., 1997. Photoinduction of UV-absorbing compounds in Antarctic diatoms and *Phaeocystis antarctica*. Mar. Ecol. Prog. Ser. 160, 13–25. https://doi.org/ 10.3354/mens160013.
- Rudels, B., Björk, G., Nilsson, J., Winsor, P., Lake, I., Nohr, C., 2005. The interaction between waters from the Arctic Ocean and the Nordic Seas north of Fram Strait and along the East Greenland Current: results from the Arctic Ocean-02 Oden expedition. J. Mar. Syst. 55, 1–30. https://doi.org/10.1016/j.jmarsys.2004.06.008.
- Sakshaug, E., Johnsen, G., Kristiansen, S., von Quillfeldt, C., Rey, F., Slagstad, D., Thingstad, F., 2009. Phytoplankton and primary production. In: Sakshaug, E., Johansen, G., Kovacs, K. (Eds.), Ecosystem Barents Sea. Tapir Academic Press, Trondheim, Norway, pp. 167–208.
- Smith Jr., W.O., Zhang, W.G., Hirzel, A., Stanley, R.M., Meyer, M.G., Sosik, H., et al., 2021. A regional, early spring bloom of *Phaeocystis pouchetii* on the New England continental shelf. J. Geophys. Res. Oceans 126 (2). https://doi.org/10.1029/ 20201C016856

- Thomalla, S.J., Nicholson, S.A., Ryan-Keogh, T.J., et al., 2023. Widespread changes in Southern Ocean phytoplankton blooms linked to climate drivers. Nat. Clim. Chang. 13, 975–984. https://doi.org/10.1038/s41558-023-01768-4.
- Tiselius, P., Belgrano, A., Andersson, L., Lindahl, O., 2015. Primary productivity in a coastal ecosystem: a trophic perspective on a long-term time series. J. Plankton Res. 38 (4), 1092–1102. https://doi.org/10.1093/plankt/fbv094.
- Vallina, S.M., Follows, M.J., Dutkiewicz, S., Montoya, J.M., Cermeno, P., Loreu, M., 2014. Global relationship between phytoplankton diversity and productivity in the ocean. Nat. Commun. 5, 4299. https://doi.org/10.1038/ncomms5299.
- Wängberg, S.-Å., Wulff, A., 2004. Impact of ultraviolet-B radiation on the development of phytoplankton communities in the eastern Atlantic sector of the Southern Ocean—results from on-deck model ecosystem experiments. Deep-Sea Res. II 51, 2731–2744. https://doi.org/10.1016/j.dsr2.2001.05.001.
- Wängberg, S.-Å., Andreasson, K.I.M., Gustavson, K., Reinthaler, T., Henriksen, P., 2008. UV-B effects on microplankton communities in Kongsfjord, Svalbard - a mesocosm experiment. J. Exp. Mar. Biol. Ecol. 365, 156–163. https://doi.org/10.1016/j. jembe.2008.08.010.
- Wassmann, P., Reigstad, M., 2011. Future Arctic Ocean seasonal ice zones and implications for pelagic-benthic coupling. Oceanography 24 (3), 220–231. https:// doi.org/10.5670/oceanog.2011.74.
- Weiss, E.L., Cape, M.R., Pan, B.J., Vernet, M., James, C.C., Smyth, T.J., Ha, S.-Y., Iriarte, J.L., Mitchell, B.G., 2022. The distribution of mycosporine-like amino acids in phytoplankton across a Southern Ocean transect. Front. Mar. Sci. 9, 1022957. https://doi.org/10.3389/fmars.2022.1022957.
- Wright, S.W., Jeffrey, S.W., 1997. High-resolution HPLC system for chlorophylls and carotenoids of marine phytoplankton. In: Jeffrey, S.W., Mantoura, R.F.C., Wright, S. W. (Eds.), Phytoplankton Pigments in Oceanography: Guidelines to Modern Methods. UNESCO, Paris, pp. 327–342.
- Yamanouchi, T., Takata, K., 2020. Rapid change of the Arctic climate system and its global influences - overview of GRENE Arctic climate change research project (2011-2016). Policy. Sci. 25, 1–47. https://doi.org/10.1016/j.polar.2020.100548.
- Zapata, M., Jeffrey, S.W., Wright, S.W., Rodriguez, F., Garrido, J.L., Clementson, L., 2004. Photosynthetic pigments in 37 species (65 strains) of Haptophyta: implications for oceanography and chemotaxonomy. Mar. Ecol. Prog. Ser. 270, 83–102. https:// doi.org/10.3354/meps270083.
- Zdun, A., Ston-Egiert, J., Ficek, D., Ostrowska, M., 2021. Seasonal and spatial changes of primary production in the Baltic Sea (Europe) based on in situ measurements in the period of 1993–2018. Front. Mar. Sci. 7, 604532.